Springer

Acta Mechanica Sinica

CrossMark click for updates

•RESEARCH PAPER•

Acta Mech. Sin., Vol. 38, 521347 (2022)
https://doi.org/10.1007/s10409-021-09029-6

Signal-to-noise ratio gain of an adaptive neuron model with Gamma renewal synaptic input

Yanmei Kang*, Yuxuan Fu, and Yaqian Chen

Department of Applied Mathematics, School of Mathematics and Statistics, Xi'an Jiaotong University, Xi'an 710049, China

Received November 1, 2021; accepted November 9, 2021; published online January 18, 2022

We take an adaptive leaky integrate-and-fire neuron model to explore the effect of non-Poisson neurotransmitter on stochastic resonance and its signal-to-noise ratio (SNR) gain. Event triggered algorithm is adopted to speed up the simulating process. It is revealed that both the output SNR and the SNR gain can be monotonically improved when increasing the shape parameter for Gamma distribution. Particularly, for large signal coupling strength, the 1:1 stochastic phase locking induced by Gamma noise is responsible for the frequency matching stochastic resonance, and the output signal-to-noise ratio can surpass the input signal-to-noise ratio, which is significantly different with Poisson case, while for extremely weak signal coupling strength, the SNR gain peak, which is far larger than unity, is due to noise induced resonance. The observations are meaningful in understanding the neural processing mechanisms from a more realistic viewpoint of synaptic modeling.

Shot noise, Gamma renewal point process, Signal-to-noise ratio gain, Adaptive integrate-and-fire model

Citation: Y. Kang, Y. Fu, and Y. Chen, Signal-to-noise ratio gain of an adaptive neuron model with Gamma renewal synaptic input, Acta Mech. Sin. **38**, 521347 (2022), https://doi.org/10.1007/s10409-021-09029-6

1. Introduction

Stochastic resonance is an unconventional phenomenon where weak coherent signal can be enhanced through operating with noise in certain circumstances [1-3], and whether the output signal-to-noise ratio (SNR) can surpass the input SNR at the optimal noise level has special significance in signal processing [4-6]. Experimental or theoretical researches on stochastic resonance have shown that noise can be utilized not only by peripheral nervous systems but also by central nervous systems. For central nervous systems, signal and noise are both coded and transmitted from the presynaptic neuron to postsynaptic neuron through action potential, namely a stereotypical electrical pulse [7,8]. Due to the random release of neurotransmitters, trains of action potential often show apparent randomness, and Poisson point process, with exponentially-distributed interarrival time, is usually chosen as the basic mathematical description of the arriving synaptic input [9,10], and in this circumstance, it has been confirmed that the SNR gain larger than one can exist with a leaky integrate-and-fire neuron model [11].

Nevertheless, abundant experimental or computational evidence from variability of spike trains shows that the Fano factor for the spike counts dramatically deviating from one [12-16], which means that Poisson point process tends to too coarse to be a realistic approximation. For example, recordings from anesthetized cat [14] revealed the Fano factor for high variability at visual cortical level can be far larger than unity, while the Fano factor for low variability in retinal, thalamic, and some cortical neurons can be much less than one. The auto-correlation analysis [17,18] for the neuronal spike trains also suggested that the neurons are more likely to fire in a non-Poisson manner. These contradictions suggest that when modeling the synaptic input it should be worthy to adopt more realistic stochastic point processes such as Gamma renewal point process [19,20].

In fact, stochastic point process is also known as shot noise, which is not only common in neural transmitter release [19,21,22] but also ubiquitous physics and engineering problems [23-25]. The Gamma renewal point process (also

*Corresponding author. E-mail address: ymkang@xjtu.edu.cn (Yanmei Kang)
Executive Editor: Guilin Wen

named Gamma noise) is one of the most important forms, and it is referred to as the type of stochastic point process with inter-arrival interval obeying Gamma distribution.

Note that Gamma distribution has two parameters: shape parameter and scale parameter, the corresponding Fano factor asymptotically approaches the reciprocal of the shape parameter, thus Gamma renewal process is capable of describing the arriving spike trains with variability ranging within a wide range. To our best knowledge, Gamma renewal process has drawn intensive attention from continuous approximation of synaptic input [19], spike sequence processing [26], fitting of interspike interval histogram [27], and formation of spiral wave [28], but how the Gamma noise affects the phenomenon of SR and its SNR is still unknown. This motivates us to examine the phenomenon of stochastic resonance and its SNR using the integrate-and-fire neuron model that transmits Gamma renewal point process.

The paper is organized as follows. In Sect. 2, adaptive leaky integrate-and-fire neuron model with the Gamma synaptic input is explained in detail. In Sect. 3, the phenomenon of stochastic resonance induced by Gamma synaptic input is explored and its SNR gain is clarified. Particularly, for large signal coupling strength, the output SNR can surpass the input SNR through frequency matching which is significantly different with Poisson case. Finally, conclusions are drawn in Sect. 4.

2. Adaptive integrate-and-fire model and Gamma shot noise

Without loss of generality, let us consider an adaptive leaky integrate-and-fire neuron model, which is a typical modification to contain the adaptive effect of the activation of adaptation ion currents, such as Ca^{2+}-activated K^+ current and Na^+-activated K^+ current in time scales from 10 ms to 1 s [29,30]. The adaptive model has dynamic rather than constant threshold and has been successfully applied to reproduce the response dynamics of individual neurons to odorant fluctuations [31].

Let $V(t)$ and $\theta(t)$ be the membrane potential and the spike threshold, respectively, then the governing equations are given by

$$\begin{cases} \tau_m \dfrac{\mathrm{d}}{\mathrm{d}t}V(t) = -\big(V(t)-V_{\mathrm{r}}\big) + w_s S(t) \\ \qquad\qquad +w_\eta \eta(t),\ V(t) < \theta(t), \\ \tau_\theta \dfrac{\mathrm{d}}{\mathrm{d}t}\theta(t) = -\theta(t) + V_{\mathrm{th}}, \quad \theta(t_0) = V_{\mathrm{th}}, \end{cases} \tag{1}$$

where V_{r} represents reversal potential, V_{th} is the constant threshold in the classical integrate-and-fire neuron model, τ_m and τ_θ are the decay constants for the membrane potential and the dynamical threshold, and t_0 is the initial time. Once the membrane potential $V(t)$ crosses the threshold $\theta(t)$ from below, an action potential is discharged, the membrane potential is immediately reset to the resting potential V_0, i.e., $V(t_+) = V_0$ and the spike threshold increases instantly by a step $\Delta\theta$, i.e., $\theta(t_+) = \theta(t_-) + \Delta\theta$, and then the membrane potential and the spike threshold restart evolution following Eq. (1). It is worthy to emphasize that when $\Delta\theta = 0$ mV Eq. (1) degenerates to a leaky integrate-and-fire model with constant threshold. Since the spike timing carries more coding information than the realistic evolution of membrane potential, the output spike train $y(t) = \sum_n \delta(t - t_n)$ with t_n standing for the nth discharge instant is taken as the output of the leaky neuron as usual and Dirac delta function $\delta(\cdot)$ to denote an instant voltage impulse.

It is reasonable to assume that the neuron receives both periodic and random input simultaneously in periodic environment such as periodic visual stimuli [32] or auditory stimuli [33,34]. Hence, in Eq. (1), $S(t) = \sum_n \delta(t - nT_s)$ is the coherent synaptic input of period T_s and coupling strength w_s. $\eta(t) = \sum_k \delta(t - t_k)$ is Gamma point process, which describes the random synaptic input with t_k being the arrival instant of the kth impulse from the presynaptic neurons, and w_η is the coupling strength. That is, the interval T between the adjacent synaptic input follows the Gamma distribution, whose probability density function is $f(t) = \dfrac{\beta^\alpha}{\Gamma(\alpha)} t^{\alpha-1} \mathrm{e}^{-\beta t} (t \geq 0)$ with α and β being shape parameter (dimensionless) and scale parameter (in Hz units), respectively as shown in Fig. 1a. The corresponding time series are displayed in Fig. 1b-d with a time window 0.01 s. According to Theorem 1 (see Appendix 1), substituting the Laplace transformation $\widetilde{f}(s) = [\beta/(\beta+s)]^\alpha$ into Eq. (A9) yields the resultant renewal strength function

$$\widetilde{m}(s) = \sum_{n=1}^{\infty} \widetilde{f}_n(s) = \sum_{n=1}^{\infty} \big(\widetilde{f}(s)\big)^n = \frac{\beta^\alpha}{(\beta+s)^\alpha - \beta^\alpha}.$$

And then with $E(T) = \alpha/\beta$ available, the spectral density of the equilibrium Gamma renewal point process $\eta(t)$ for each $f \neq 0$ reads

$$\Phi_\eta(f) = \frac{\beta}{2\pi\alpha}\left[1 + \frac{\beta^\alpha}{(\beta+2\pi \mathrm{i} f)^\alpha - \beta^\alpha} + \frac{\beta^\alpha}{(\beta-2\pi \mathrm{i} f)^\alpha - \beta^\alpha}\right]. \tag{2}$$

The power spectral densities of Gamma synaptic input which have the same parameters as Fig. 1 are displayed in Fig. 2.

In the investigation of stochastic resonance, the coherent synaptic input can be cataloged into subthreshold if it cannot emit action potential by itself; otherwise, it is superthreshold. Here we emphasize that conventionally it tends to believe

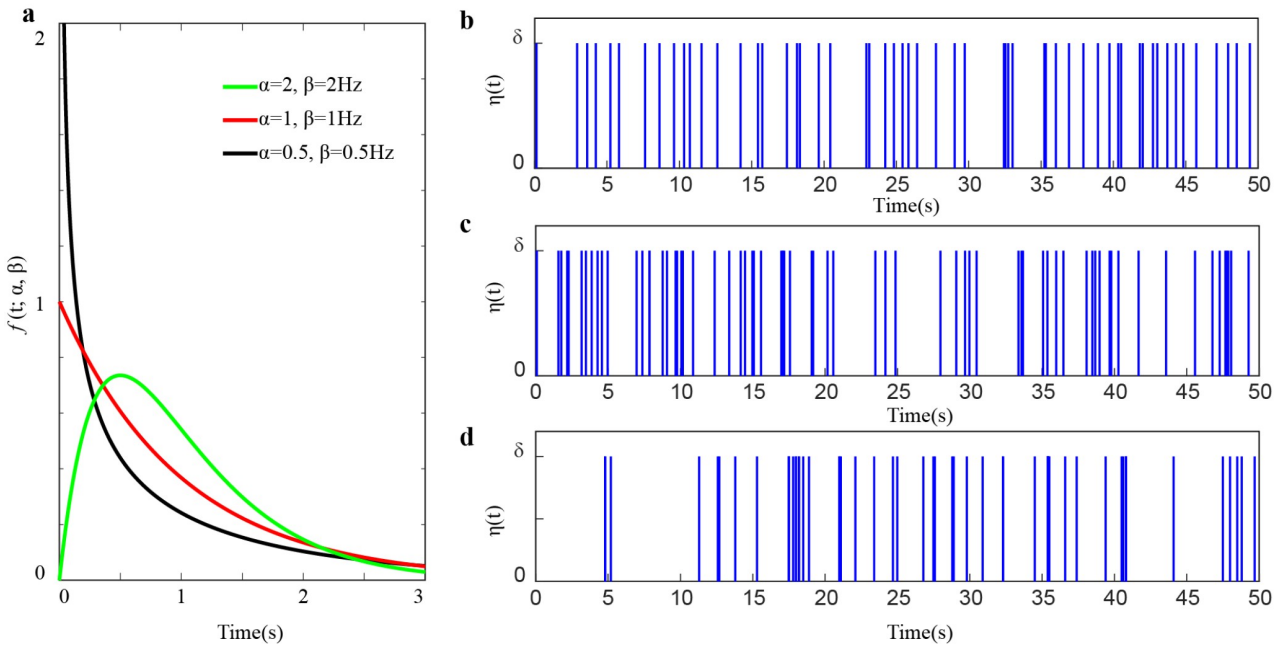

Figure 1 An intuitive demonstration of Gamma renewal point process. **a** shows the probability density curves of Gamma distribution with different parameters and **b-d** display the time series of Gamma renewal point process which correspond to the green, red, and black curves of **a** in order. In particular, the sample **c** is the conventional Poisson point process.

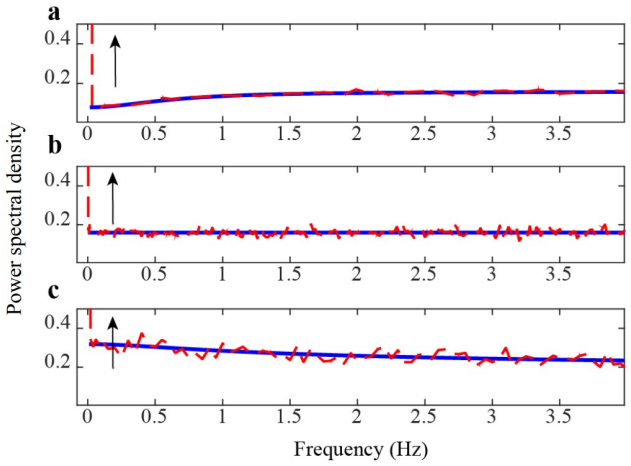

Figure 2 Power spectral density of equilibrium Gamma renewal point process with upward arrow indicating the infinite spike spectral line at zero frequency. The curves demonstrate that the theoretical power spectral density (blue solid) and the simulated counterparts (red dashed line) agree well with each other under all the cases: **a** $\alpha = 2$, $\beta = 2$ Hz, **b** $\alpha = 1$, $\beta = 1$ Hz, and **c** $\alpha = 0.5$, $\beta = 0.5$ Hz.

that the subthreshold signal is useless, and it is stochastic resonance that totally changes this obsolete point, since the information carried by subthreshold signal can be transmitted to the other neurons under the assistance of noise ubiquitous in nervous systems, as confirmed by many biophysical experiments [1]. Here we remark that the upper bound of subthreshold signal coupling strength for Eq. (1) is the same as that for the constant threshold model [9], i.e.,

$$\widehat{w}_s = \tau_m V_{\text{th}}\left[1 - \exp\left(T_s / \tau_m\right)\right],$$

when the resting potential V_0 vanishes, since the threshold always stays V_{th} before the first spike is emitted. That is, when $w_s < \widehat{w}_s$, the coherent input signal fails to emit any action potential by itself and thus noise becomes an indispensable factor for neural transmission. Biologically, the voltage of the pyramidal neuron will enhance 0.2-6 mV when the presynaptic spike arrives [35,36], which means that w_s and w_η should be taken values within $[0.2,\ 6] \cdot \tau_m$ to be consistent with the biophysical observation.

In this paper, we fix $\tau_m = 20$ ms, $\tau_\theta = 100$ ms, $\Delta\theta = 2$ mV, $V_r = V_0 = 0$ mV [31], $T_s = 200$ ms, and the simulation time span $T = 2 \times 10^6$ ms, unless otherwise stated. Note that the noise intensity of Gamma renewal point process, namely the arrival frequency of the incoming spikes, can be obtained by the shape parameter α and the scale parameters β as β / α. When the frequency is low, to avoid the huge amount of simulation time cost by Euler-Maruyama scheme, we present a four-step event triggered algorithm as shown in Appendix 2. Our numerical experience indeed shows that the event triggered algorithm is much more effective in the case of weak noise.

3. Stochastic resonance and its SNR gain

Subthreshold signal itself alone cannot be transmitted, but it becomes transmissible under the assistance of noise as shown in Fig. 3. From the picture, it is clear that the (Gamma) noise assisted firing might randomly occur at some integer multiple of the signal period T_s, that is, the output

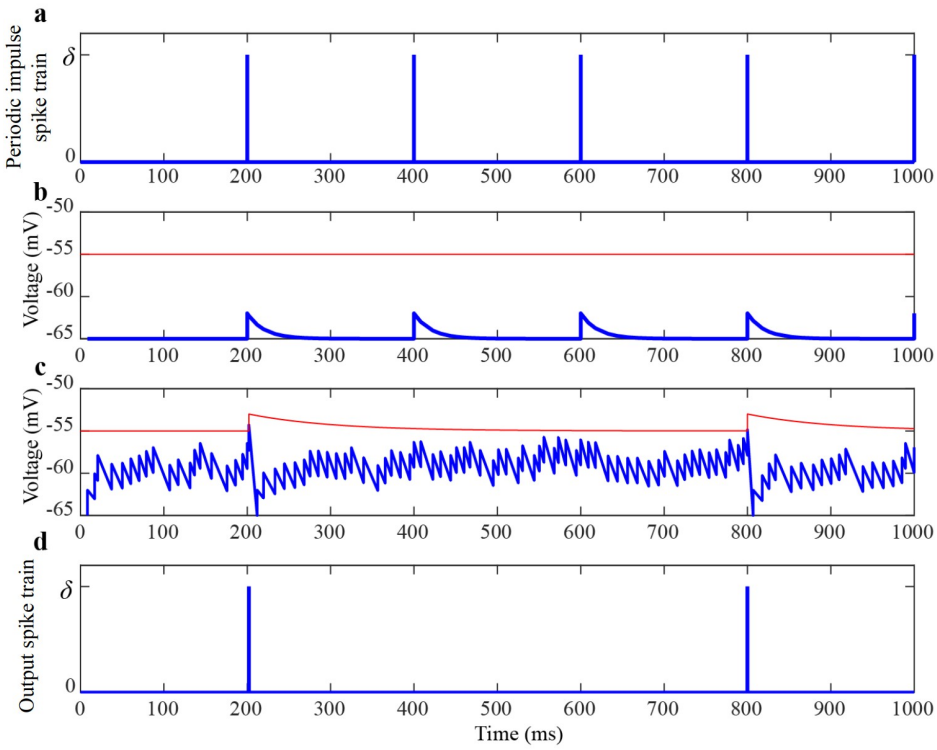

Figure 3 The evolution of periodic impulsive input, membrane potential, and output spike train. **a** presents the periodic input; **b** exhibits the potential variation $V(t)$ when ignoring the noise, **c** exhibits the potential variation with Gamma noise, and **d** shows the corresponding output train. The red curves in **b** and **c** denote the threshold. The parameters are $w_s = w_\eta = 0.5\widehat{w}_s$, $\alpha = 10$, and $\beta = 1$ Hz.

spike train carries the characteristic of the weak subthreshold stimulus. Thus, Gamma noise plays a positive role in neural transmission, while the phenomenon of stochastic resonance to be explored below further demonstrates that such transmission can be optimally maximized at suitable noise intensity. Note that for Gamma renewal point process of shape parameter α and scale parameter β, although the noise intensity of Gamma noise is β/α, the resultant Fano factor is $1/\alpha$. Thus we explore the effect of Gamma noise on stochastic resonance for the varying α, and for each α we adjust the noise intensity by changing the scale parameter β.

The SNR is one of the most frequently used indices for quantifying the phenomenon of stochastic resonance, and the bell-shape curve of the output SNR via noise intensity signifies the occurrence of stochastic resonance. Following Refs. [7,11,14], the output SNR can be defined as

$$R_{\text{out}} = P_{\text{out}}(1/T_s)/N_{\text{out}}(1/T_s), \tag{3}$$

where $P_{\text{out}}(f)$ denotes the power spectral density of the noisy output spike train. The numerator represents its periodic signal component, and the denominator denotes the power spectral density of noise at the frequency of the periodic component. The noise power spectral density $N_{\text{out}}(1/T_s)$ is estimated by averaging 40 spectral lines $P_{\text{out}}(f)$ around the fundamental frequency but not including $P_{\text{out}}(1/T_s)$. Similarly, for the noisy synaptic input $w_s S(t) + w_\eta \eta(t)$, the input SNR is defined as

$$R_{\text{in}} = \frac{P_{\text{in}}(1/T_s)}{N_{\text{in}}(1/T_s)} = \frac{w_s^2}{w_\eta^2} \cdot \frac{P_S(1/T_s)}{P_\eta(1/T_s)}, \tag{4}$$

where $P_{\text{in}}(f)$, $P_S(f)$, and $P_\eta(f)$ are the power spectral density of the noisy input spike train, coherent signal $S(t)$, and Gamma input $\eta(t)$. The noise component $N_{\text{in}}(1/T_s)$ can be acquired by two methods. The first one is to multiply w_η^2 and $P_\eta(1/T_s)$ which is obtained by Eq. (2) analytically. The second one is to directly calculate it in the same way as that for $N_{\text{out}}(1/T_s)$ numerically. We emphasize that the two methods are consistent, as confirmed in Fig. 2. Further, according to Eqs. (3) and (4), the SNR gain is given by

$$G = R_{\text{out}}/R_{\text{in}}. \tag{5}$$

On the other hand, we adopt the average firing rate to provide an explanation of stochastic resonance from physical mechanism. The average firing rate is defined as

$$r = \int_0^{T_{\text{span}}} \langle y(t) \rangle \mathrm{d}t / T_{\text{span}}, \tag{6}$$

which equals to the reciprocal of mean interspike interval (when the refractory period is omitted). As is known, the output SNR can describe the involving coherence to some extent, while the average firing rate is totally a rate coding tool [36,37]. Although the average firing rate cannot reflect the temporal pattern, it can be used to explain the physical

mechanism of stochastic resonance from phase locking or deterministic resonance. Hence, we combine these indices to have an in-depth understanding on the effect of stochastic resonance induced by Gamma noise.

Figure 4 shows the evolution of the SNR (3), the SNR gain (5), and the firing rate (6) via noise intensity under different shape parameter α. The non-monotonic SNR curves in Fig. 4a, d, and g identify the characteristic of stochastic resonance: the peak of the output SNR curve becomes higher as the shape parameter α increases. This observation means the less Fano factor, the higher SNR. For example, if we take the output SNR of the Poisson noise case ($\alpha = 1$) as the benchmark, when Gamma case becomes Erlang manner with $\alpha = 10$, the output SNR at the optimal noise intensity attains 1.69 times. Moreover, the SNR gain at the optimal noise intensity shows a similar trend: the less Fano factor, the higher SNR gain, although the SNR gain can surpass one only when alpha is larger enough. Surprisingly, the SNR gain in Fig. 4b and e does not show a peak at the optimal noise intensity as that in Fig. 4h, and in fact, the SNR gain monotonically grows as the noise intensity increases. These behaviors together with the observation in Ref. [11] imply that Eq. (1) is actually a signal amplifier when the Fano factor is smaller than one. By further checking the evolution of firing rate as shown in Fig. 4c, f, and i, we find that the average firing rates are quite similar for the Poisson case and Gamma case. Therefore, according to the principle of energy minimization [38,39], Gamma synaptic input with a large alpha is more suitable for neuron transmission supposing that the energy demand for a single spike is constant.

To deepen the above observation and discussion which have exhibited the influence of Gamma noise on signal transmission, we fix $\alpha = 10$ but take w_s and w_η tunable. Figure 5 shows that the output SNR can be boosted by increasing the signal coherent coupling strength or decreasing the noise coupling strength. However, the SNR gain curves no longer display a monotonic trend for the varying w_s and w_η. Therefore, in order to obtain a comprehensive understanding on the variation of SNR gain, we draw the pseudo color image of SNR gain at the occurrence of SR within a range of physiologically meaningful parameters, $w_s \times w_\eta = [0.1,\ 0.6]\widehat{w}_s \times [0.1,\ 0.6]\widehat{w}_s$ in Fig. 6a. Obviously, there are two SNR gain peaks. The one is near point A, representing an extremely weak w_s but strong w_η area. The other one is near point B, representing a larger.

The aforementioned two peaks also appear in the case of Poisson noise case [11]. It can be found that the physical mechanisms underlying the two peaks are different. In fact, by checking the average firing rate at the optimal noise intensity, we find that for a larger coherent coupling w_s, the average firing rate at the best noise intensity is around 5 Hz

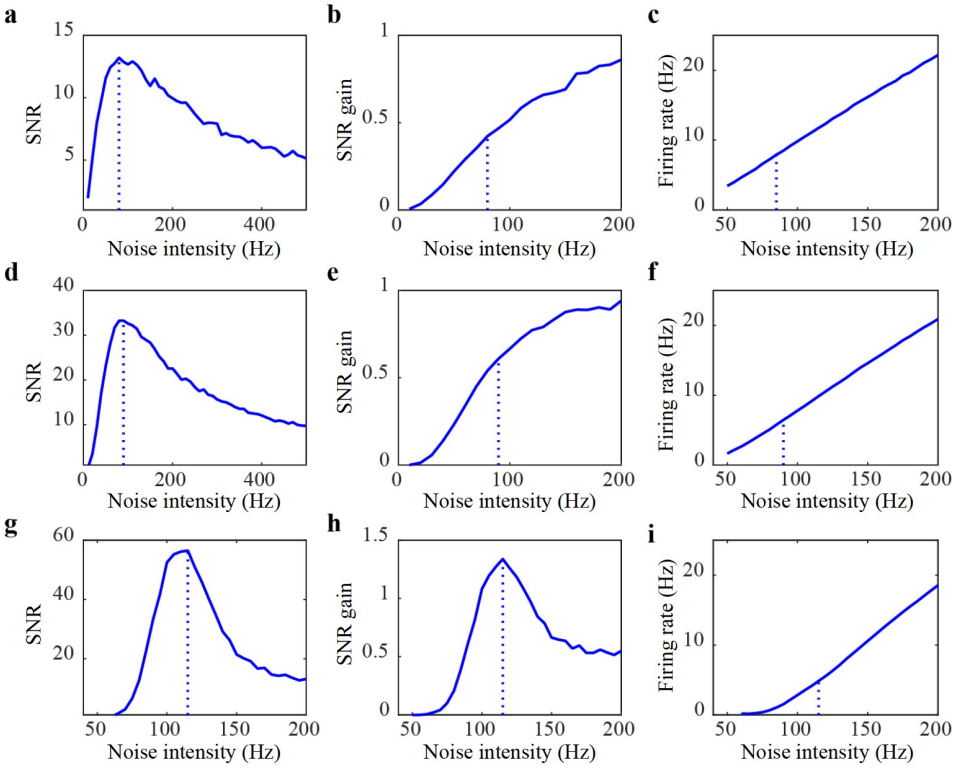

Figure 4 SNR (left), the corresponding gain (middle), and the corresponding firing rate (right) versus noise intensity with $\alpha = 0.5$ **a-c**, $\alpha = 1$ **d-f**, and $\alpha = 10$ **g-i**. The coupling strengths are $w_s = w_\eta = 0.3\widehat{w}_s$. The vertical dotted line denotes optimal noise intensity parameter, which clearly shows: the larger the alpha, the higher the optimal noise level.

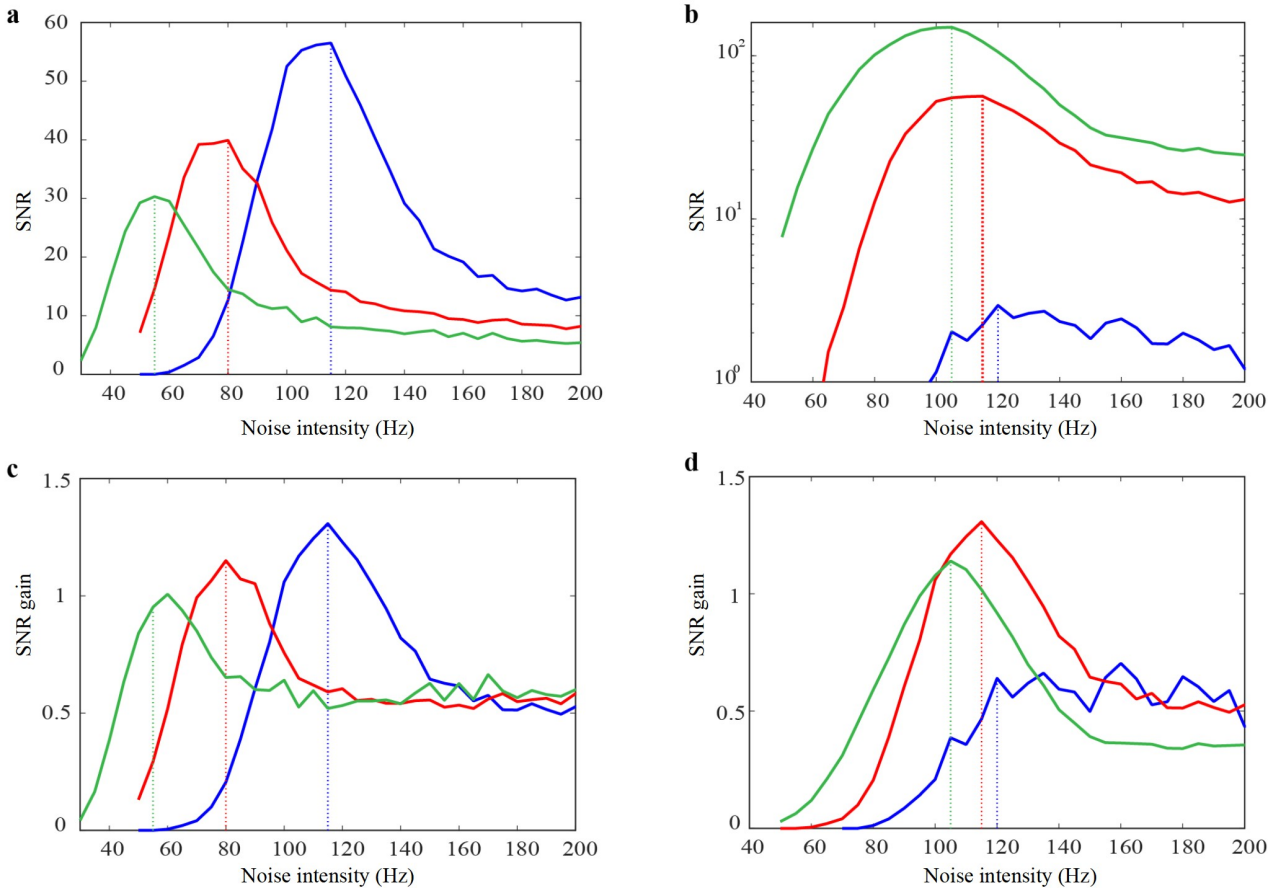

Figure 5 Dependence of the output SNR **a**, **b** and SNR gain **c**, **d** on noise intensity with $\alpha = 10$. The parameters for the first column are $w_s = 0.3\hat{w}_s$ and $w_\eta = 0.3\hat{w}_s$ (blue), $w_\eta = 0.4\hat{w}_s$ (red), $w_\eta = 0.5\hat{w}_s$ (green). The parameters for the second column are $w_\eta = 0.3\hat{w}_s$, $w_s = 0.1\hat{w}_s$ (blue), $w_s = 0.3\hat{w}_s$ (red), $w_s = 0.5\hat{w}_s$ (green). The vertical dotted line denotes optimal noise intensity parameter.

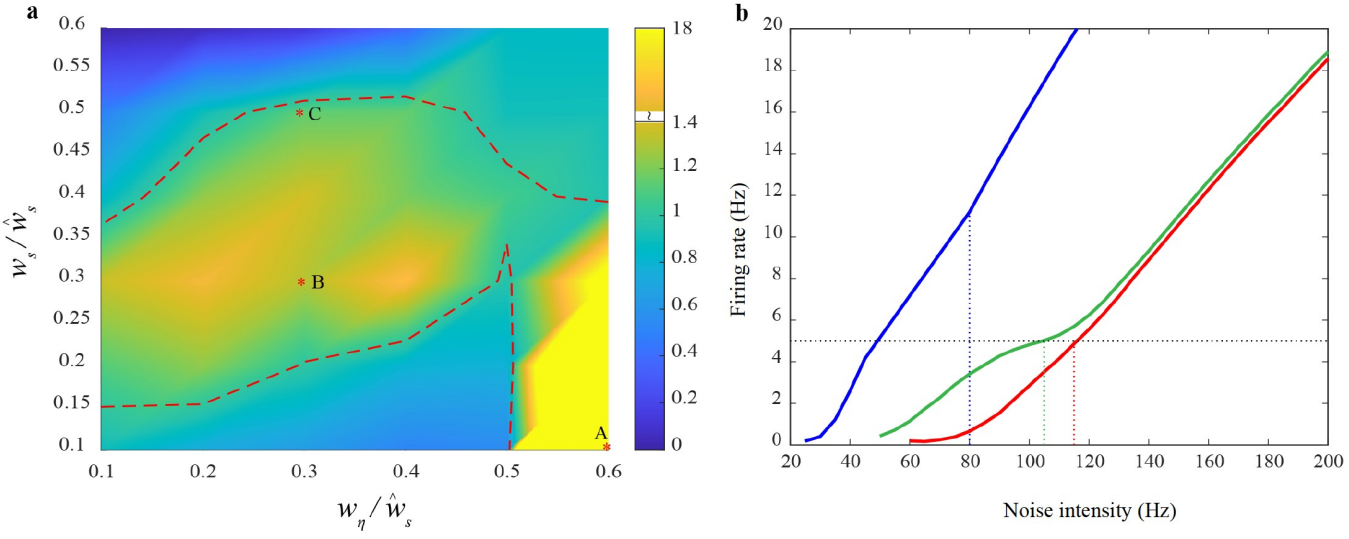

Figure 6 **a** Pseudo color image of SNR gain at the occurrence of SR for the varying w_s and w_η with $\alpha = 10$. The red dashed curve is the contour line at which SNR gain equals to unity. It shows that both the central region and the bottom right region have the local SNR gain peak and the peak values are larger than unity. **b** Dependence of the firing rate on noise intensity for the varying $w_s = 0.1\hat{w}_s$, $w_\eta = 0.6\hat{w}_s$ (blue), $w_s = 0.3\hat{w}_s$, $w_\eta = 0.3\hat{w}_s$ (red), and $w_s = 0.5\hat{w}_s$, $w_\eta = 0.3\hat{w}_s$ (green). The blue, red, and green curves correspond to points A, B, and C in **a**, respectively. The vertical dotted line denotes optimal noise intensity parameter, and the horizontal dotted line denotes the frequency of the input signal.

as shown in Fig. 6b (red and green curves), thus it is consistent with frequency of the input signal, i.e., $r = F_{\text{input}} = 1 / T_s$, which means that the phenomenon of stochastic resonance in this case is caused by a stochastic phase lock similar frequency-matching mechanism [11,40]. At this moment, although the role of the synaptic noise is necessary, the event of $V(t)$ reaching the threshold is dominated by the coherent signal, thus the peak of SNR gain moves to the center area of the considered range, namely point B $(w_s, w_\eta) = (0.3\widehat{w}_s, 0.3\widehat{w}_s)$. However, for an extremely weak w_s but strong w_η, this kind of frequency-matching relationship disappears, and thus the phenomenon of SR should owe to noise-induced resonance, as observed from Fig. 6b (blue curve). In this case, whether $V(t)$ can reach the spike threshold is nearly completely dominated by the synaptic noise. The noise energy converts heavily into the power component of the output at the signal frequency $1 / T_s$, causing the significant rise of SNR gain to occur. At last, we emphasize that not only in the area near A but also near B, the SNR gain can be larger than one due to the more generality of Gamma distribution, which is significantly different from the Poisson case [11]. Therefore, our observation in this paper actually illustrates the variety of Gamma noise induced stochastic resonance.

Finally, the influence of decay constants τ_m on both SNR and SNR gain is further investigated. Other parameters are selected near point B in Fig. 6 where the SNR gain is significantly different for Poisson type and Gamma type synaptic input. Figure 7 shows that the SNRs are almost same at the optimal noise intensity, but SNR gain will monotonically decrease with the increasing τ_m. The underlying reason can be found from the frequency-matching mechanism. According to Eq. (1), the membrane potential $V(t)$ decays at a rate of $\exp(-t / \tau_m)$. Thus, the higher τ_m is, the slower the attenuation speed of the voltage is, which results in the rise of firing rate. Based on the frequency-matching mechanism, the optimal noise intensity whose corresponding firing rate reaches $1 / T_s$ will shift to the left as shown in Fig. 7a, d, and g, and the input SNR will increase accordingly. Therefore, the SNR gain will monotonically decrease eventually.

4. Conclusion

We have explored the cooperative dynamics of the Gamma renewal neurotransmitter release and the subthreshold periodic impulse input in an adaptive integrate-and-fire neuron model by event triggered simulation algorithm. In order to obtain an explicit expression for the input SNR, we revisited the spectral property of an equilibrium Gamma renewal point process. In the sense that the input SNR and the output SNR

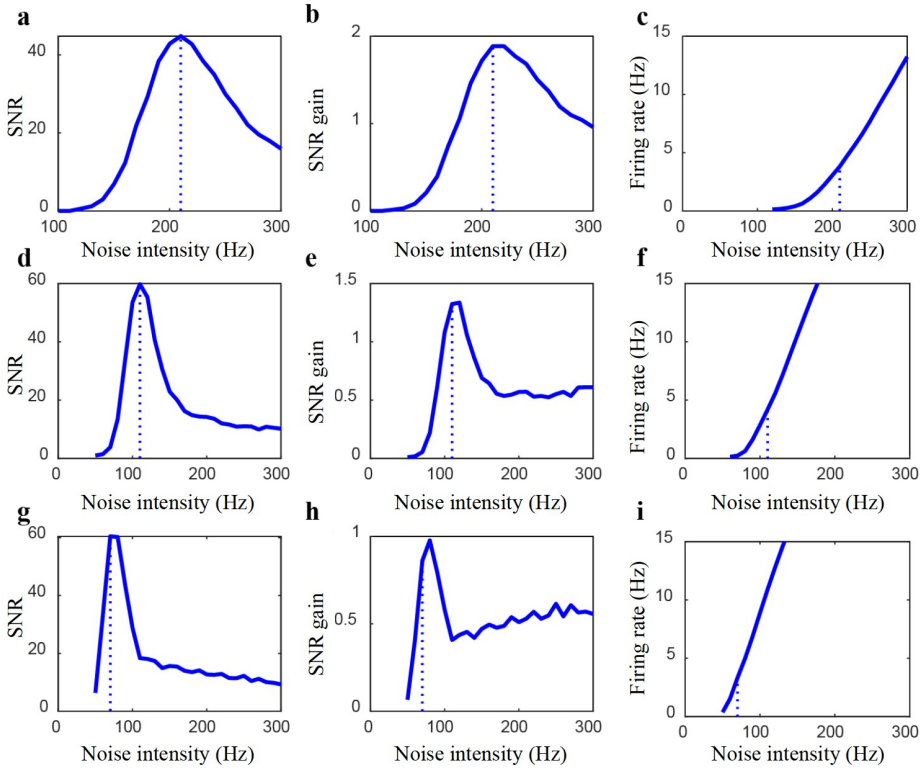

Figure 7 SNR (left), the corresponding gain (middle), and the corresponding firing rate (right) versus noise intensity with τ_m = 10 ms **a-c**, τ_m = 20 ms **d-f**, and τ_m = 30 ms **g-i**. The coupling strengths are $w_s = w_\eta = 0.3\widehat{w}_s$ and the shape parameter is $\alpha = 10$. The vertical dotted line denotes optimal noise intensity parameter, which clearly shows: the larger τ_m, the smaller the SNR gain.

are both calculated consistently with a high accuracy, the phenomenon of stochastic resonance induced by Gamma noise is disclosed, and the SNR gain is exhibited.

From our investigation, it is found again that there are two kinds of physical mechanisms responsible for the stochastic resonance, the noise-induced resonance, and the stochastic phase-locking similar frequency-matching resonance. Particularly, we found that reducing the Fano factor or increasing the shape parameter contributes to a better SNR gain and the SNR gain at the optimal noise intensity can exceed one eventually. For a large, there are two SNR gain peaks which correspond to the aforementioned two kinds of physical mechanisms, respectively. One of them is located at extremely weak signal coherent coupling but strong noise coupling region, namely, the other one is near. Using the frequency-matching mechanism, we explain the phenomenon that the SNR gain will monotonically increase with the decreasing decay constant τ_m. These findings discover that the neuron indeed becomes a signal amplifier with Gamma renewal neurotransmitter release and thus are meaningful for both biological modeling research and artificial neural network design. In future, we will consider the stochastic resonance behavior in the neural network under gamma synaptic input, mainly focusing on the effects of both network structure and gamma shot noise on SNR and SNR gain, and design the corresponding applications based on the dynamical studies.

This work was supported by the Non-Poisson Modeling of Neuron Synaptic Input and Critical Dynamics for Cortical Networks (Grant No. 11772241).

1 L. Gammaitoni, P. Hänggi, P. Jung, and F. Marchesoni, Stochastic resonance, Rev. Mod. Phys. **70**, 223 (1998).
2 L. Q. Uddin, Bring the noise: reconceptualizing spontaneous neural activity, Trends Cogn. Sci. **24**, 734 (2020).
3 Y. Xu, Y. Guo, G. Ren, and J. Ma, Dynamics and stochastic resonance in a thermosensitive neuron, Appl. Math. Comput. **385**, 125427 (2020).
4 G. Winterer, M. Ziller, H. Dorn, K. Frick, C. Mulert, N. Dahhan, W. M. Herrmann, and R. Coppola, Cortical activation, signal-to-noise ratio and stochastic resonance during information processing in man, Clin. Neurophysiol. **110**, 1193 (1999).
5 Z. Gingl, P. Makra, and R. Vajtai, High signal-to-noise ratio gain by stochastic resonance in a double well, Fluct. Noise Lett. **01**, L181 (2001).
6 P. Makra, and Z. Gingl, A dynamical system exhibits high signal-to-noise ratio gain by stochastic resonance, Am. Inst. Phys. **7**, 100 (2003).
7 L. Zhangcai, and Q. Youguo, Stochastic resonance driven by time-modulated neurotransmitter random point trains, Phys. Rev. Lett. **91**, 208103 (2003).
8 J. D. Touboul, C. Piette, L. Venance, and G. B. Ermentrout, Noise-induced synchronization and antiresonance in interacting excitable systems: applications to deep brain stimulation in parkinson's disease, Phys. Rev. X **10**, 011073 (2020).
9 A. N. Burkitt, A review of the integrate-and-fire neuron model: I. Homogeneous synaptic input, Biol. Cybern. **95**, 1 (2006).
10 A. N. Burkitt, A review of the integrate-and-fire neuron model: II. Inhomogeneous synaptic input and network properties, Biol. Cybern. **95**, 97 (2006).
11 Y. M. Kang, J. X. Xu, and Y. Xie, Signal-to-noise ratio gain of a noisy neuron that transmits subthreshold periodic spike trains, Phys. Rev. E **72**, 021902 (2005).
12 A. Amarasingham, T. L. Chen, S. Geman, M. T. Harrison, and D. L. Sheinberg, Spike count reliability and the poisson hypothesis, J. Neurosci. **26**, 801 (2006).
13 A. A. Faisal, L. P. J. Selen, and D. M. Wolpert, Noise in the nervous system, Nat. Rev. Neurosci. **9**, 292 (2008).
14 P. Kara, P. Reinagel, and R. C. Reid, Low response variability in simultaneously recorded retinal, thalamic, and cortical neurons, Neuron **27**, 635 (2000).
15 G. Maimon, and J. A. Assad, Beyond poisson: increased spike-time regularity across primate parietal cortex, Neuron **62**, 426 (2009).
16 K. Rajdl, and P. Lansky, Stein's neuronal model with pooled renewal input, Biol. Cybern. **109**, 389 (2015).
17 H. Cĝteau, and A. D. Reyes, Relation between single neuron and population spiking statistics and effects on network activity, Phys. Rev. Lett. **96**, 058101 (2006).
18 B. Lindner, Superposition of many independent spike trains is generally not a Poisson process, Phys. Rev. E **73**, 022901 (2006).
19 J. Feng, Y. Deng, and E. Rossoni, Dynamics of moment neuronal networks, Phys. Rev. E **73**, 1 (2006).
20 P. Lansky, L. Sacerdote, and C. Zucca, The Gamma renewal process as an output of the diffusion leaky integrate-and-fire neuronal model, Biol. Cybern. **110**, 193 (2016).
21 J. Bauermann, and B. Lindner, Multiplicative noise is beneficial for the transmission of sensory signals in simple neuron models, Biosystems **178**, 25 (2019).
22 M. Tamborrino, and P. Lansky, Shot noise, weak convergence and diffusion approximations, Phys. D-Nonlinear Phenom. **418**, 132845 (2021).
23 I. Eliazar, and J. Klafter, On the nonlinear modeling of shot noise, Proc. Natl. Acad. Sci. USA **102**, 13779 (2005).
24 Q. Chen, and N. Xu, Shot noise in superconducting wires applied with a periodic electric field, J Nanosci. Nanotechnol. **18**, 3729 (2017).
25 H. X. Lü, and Z. W. Xie, The shot noise in quasi one-dimensional magnetic tunnel junctions, Sci. Sin.-Phys. Mech. Astron. **48**, 057501 (2018).
26 T. Marc, When less is more: Non-monotonic spike sequence processing in neurons, Front. Comput. Neurosci. **5**, (2011).
27 S. R. Seydnejad, Reconstruction of the input signal of the leaky integrate-and-fire neuronal model from its interspike intervals, Biol. Cybern. **110**, 3 (2016).
28 Y. Kang, Y. Chen, Y. Fu, Z. Wang, and G. Chen, Formation of spiral wave in Hodgkin-Huxley neuron networks with Gamma-distributed synaptic input, Commun. Nonlinear Sci. Numer. Simul. **83**, 105112 (2020).
29 J. Benda, L. Maler, and A. Longtin, Linear versus nonlinear signal transmission in neuron models with adaptation currents or dynamic thresholds, J. Neurophysiol. **104**, 2806 (2010).
30 C. Yuan, and J. Wang, Comparison of firing mechanisms of neuron model adaptability under external alternating electric field, J. Northeast. Univ. **35**, 1229 (2014).
31 M. Levakova, L. Kostal, C. Monsempès, P. Lucas, and R. Kobayashi, Adaptive integrate-and-fire model reproduces the dynamics of olfactory receptor neuron responses in a moth, J. R. Soc. Interface. **16**, 20190246 (2019).
32 F. B. Vialatte, M. Maurice, J. Dauwels, and A. Cichocki, Steady-state visually evoked potentials: Focus on essential paradigms and future perspectives, Prog. Neurobiol. **90**, 418 (2010).
33 U. Will, and E. Berg, Brain wave synchronization and entrainment to periodic acoustic stimuli, Neurosci. Lett. **424**, 55 (2007).
34 A. Schilling, K. Tziridis, H. Schulze, and P. Krauss, The stochastic resonance model of auditory perception: A unified explanation of tinnitus development, Zwicker tone illusion, and residual inhibition, Prog. Brain Res. **262**, 139 (2021).

35 H. Markram, J. Lübke, M. Frotscher, A. Roth, and B. Sakmann, Physiology and anatomy of synaptic connections between thick tufted pyramidal neurones in the developing rat neocortex, J. Physiol. **500**, 409 (1997).
36 M. J. E. Richardson, and R. Swarbrick, Firing-rate response of a neuron receiving excitatory and inhibitory synaptic shot noise, Phys. Rev. Lett. **105**, 178102 (2010).
37 W. Gerstner, W. M. Kistler, R. Naud, and L. Paninski, Neuronal dynamics: From single neurons to networks and models of cognition (Cambridge University Press, Cambridge, 2014).
38 S. B. Laughlin, and T. J. Sejnowski, Communication in neuronal networks, Science **301**, 1870 (2003).
39 F. Zhu, R. Wang, X. Pan, and Z. Zhu, Energy expenditure computation of a single bursting neuron, Cogn. Neurodyn. **13**, 75 (2019).
40 Y. M. Kang, J. X. Xu, and Y. Xie, A further insight into stochastic resonance in an integrate-and-fire neuron with noisy periodic input, Chaos Solitons Fractals **25**, 165 (2005).

伽马更新突触输入作用下自适应神经元模型的信噪比增益

康艳梅, 付宇轩, 陈亚倩

摘要 我们采用自适应漏电积分-放电模型来研究非泊松递质对随机共振及其信噪比增益的影响, 并运用事件驱动算法加速模拟过程. 研究结果表明, 输出信噪比和信噪比增益都会随着伽马分布的形状参数的增加而增加. 特别地, 当输入信号幅值较大时, 由Gamma噪声诱导的1:1随机锁像揭示出此时发生的是满足频率匹配关系的随机共振现象, 并且输出信噪比可以超过输入信噪比, 这与Poisson情形显著不同; 而当输入信号幅值极弱时, 信噪比增益会远远大于1, 这是由于发生了噪声诱导的随机共振现象. 这些观察结果对于从更现实的突触建模角度理解神经信息处理机制是有意义的.